

RSC Advances



This is an *Accepted Manuscript*, which has been through the Royal Society of Chemistry peer review process and has been accepted for publication.

Accepted Manuscripts are published online shortly after acceptance, before technical editing, formatting and proof reading. Using this free service, authors can make their results available to the community, in citable form, before we publish the edited article. This *Accepted Manuscript* will be replaced by the edited, formatted and paginated article as soon as this is available.

You can find more information about *Accepted Manuscripts* in the [Information for Authors](#).

Please note that technical editing may introduce minor changes to the text and/or graphics, which may alter content. The journal's standard [Terms & Conditions](#) and the [Ethical guidelines](#) still apply. In no event shall the Royal Society of Chemistry be held responsible for any errors or omissions in this *Accepted Manuscript* or any consequences arising from the use of any information it contains.

A Microfluidic-based Controllable Synthesis of Rolling or Rigid Ultrathin Gold Nanoplates

Qiang Fu, Guangjun Ran, and Weilin Xu*

State Key Laboratory of Electroanalytical Chemistry, & Jilin Province Key Laboratory of Low Carbon Chemical Power, Changchun Institute of Applied Chemistry, Chinese Academy of Science, 5625 Renmin Street, Changchun 130022, P.R. China.

*E-mail: weilinxu@ciac.ac.cn

Abstract: A continuous microfluidic-based seed-mediated synthesis of high-purity gold nanoplates with different thickness was developed. The thickness of the nanoplates can be fairly tuned from less than 1 nm to a few nm by varying the flow rate. Depend on the thickness, the obtained nanoplates could be rigid and surface-flat with thickness larger than 2 nm or flexible with crumpling or rolling shapes when the thickness is around 1 nm. These nanoplates are poly-crystalline with different crystal faces and show a great electrochemical activity toward glucose oxidation.

Introduction

The control of metal nanostructure morphology (size, shape, and surface structure) has attracted much attention in recent years due to the interest in precise tuning of electronic, optical, and catalytic properties.¹⁻⁴ Consequently, a variety of nonspherical gold nanocrystals with different shapes such as rods,^{5, 6} wires,^{7, 8} belts,^{9, 10} comb,¹⁰ plates and prism,^{11, 12} polyhedral,¹³⁻¹⁷ cages and frames,¹⁸ caps,¹⁹ stars and flowers,²⁰⁻²⁴ as well as dendrites²⁵⁻²⁹ have been achieved. However, these various types of nanocrystals were almost obtained by bench top batch preparative methods which are successful in laboratory. These methods are not convenient on the synthesis of anisotropic nanocrystals at large scale. Therefore, microfluidic methods have been regarded as suitable alternative protocols with a high possibility to gain large quantities of

particles with a uniform size and shape continuously.^{30, 31} Also, among the gold nanocrystals discussed above, microfluidic protocols have been used to prepare for various shapes of nanoparticles with different sizes (e. g. spherical nanoparticles, nanorods, hexagonal and triangular nanoplates and so on).^{30, 32-39} As for gold nanoplates, to our best knowledge, no one have already successfully prepared gold nanoplates with different thickness by the microfluidic protocol although similar protocol has been used for synthesis of size-different gold nanoparticles.³⁶ Although various bench top batch preparative methods have been reported for the synthesis of gold nanoplates with or without bending contour,^{12, 40-42} these gold nanoplates are mainly have sizes in the micrometer range and thicknesses of tens of nanometers with a mixed shapes of obtuse triangle, hexagon, quasi-round and so on. Furthermore, the evitable co-existence of a large number of ball-like nanoparticles during these methods is really a waste of gold sources which is limited on the earth.

Recently, we reported a continuous microfluidic-based synthesis of Au supraparticles.⁴³ In that work, it was revealed that a type of flexible thin Au nanoplate is in fact the first intermediate for the growth of Au supraparticles. Herein, by varying the flow rate in the microfluidic device, we obtained a series of Au nanoplates with controllable thickness and found the morphology (rolling or rigid) of the Au nanoplates could be tuned by controlling the thickness of the nanoplates. In addition, the

electrochemical test shows that the electrocatalytic activity of the nanoplates toward glucose oxidation depends on the morphology of the nanoplates: the rolling ones show much higher catalytic activity than the flat ones.

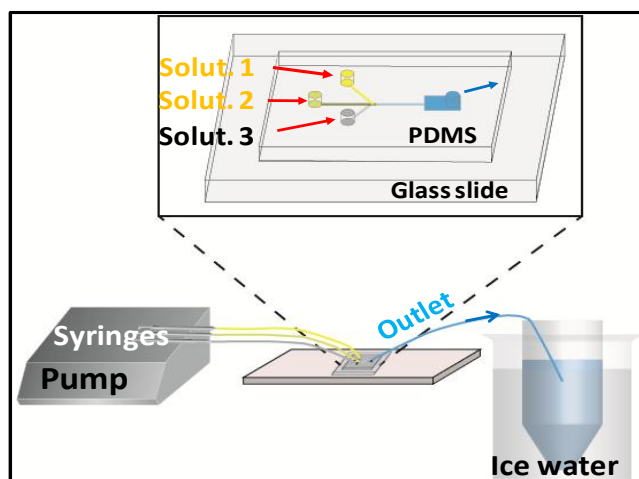
Experimental section

Chemicals. Hydrogen tetrachloroaurate trihydrate ($\text{HAuCl}_4 \cdot 3\text{H}_2\text{O}$) was purchased from Sigma-Aldrich. Cetyltrimethylammonium chloride (CTAC), sodium borohydride (NaBH_4), and ascorbic acid (AA) were purchased from Shanghai Sinopharm Chemical Reagent Co., Ltd. Sodium bromide (NaBr), β -D-glucose, sulphuric acid (H_2SO_4), and potassium hydrogen phosphate (KH_2PO_4 and K_2HPO_4) were purchased from Beijing Chemical Co.. All chemicals were used as received without further purification. Ultrapure distilled water ($18.2 \text{ M}\Omega$) was used for all solution preparations.

Synthesis of Gold Seeds. A volume of 10 mL aqueous solution containing $2.5 \times 10^{-4} \text{ M}$ HAuCl_4 and 0.10 M CTAC was prepared first. Then, 0.45 mL of the NaBH_4 solution (0.02 M, ice-cold) was added into the above solution with stirring. The resulting solution turned brown immediately, indicating the formation of gold seeds, which were aged for 1 h at 30°C to decompose excess borohydride. The seed particles have a size of about 4 nm (Fig. S1).

Microfluidic synthesis of gold nanoplate

The microfluidic chip consists of a microchannel ($400\ \mu\text{m} \times 400\ \mu\text{m}$ cross-section and 3 cm long) with three inlets and one outlet.⁴³ As shown in scheme 1 and Fig. S2. The reaction regime was divided into three different solutions: **Solution 1**: 375 μL of 0.01 M HAuCl_4 solution, 15 μL of 0.01 M NaBr solution and 4.6 mL of 0.1 M CTAC solution were mixed together; **Solution 2**: 135 μL of 0.04 M ascorbic acid solution and 4.8 mL of 0.1 M CTAC solution were added together; **Solution 3**: 150 μL seed solution and 4.8 mL of 0.1 M CTAC solution were taken together. Then these three different solutions were injected into the microfluidic chip through three independent channels at the same rate. Meanwhile, the effluent from the chip was collected into a centrifugal tube with large amount of ice-cold ultrapure water to terminate the growth. The solution in the tube was then centrifuged at 12000 rpm for at least 15 min. To remove the excessive surfactant, the precipitate was washed by water twice through centrifugation at 12000 rpm for no less than 15 min. By varying the flow rate of solution, nanoplates with different thickness were obtained.



Scheme 1. The setup of the flow-based microfluidic system for synthesis of the ultrathin gold nanoplate.

Preparation of gold nanoplates-modified electrode. Glassy carbon electrode (GCE) was polished before each experiment with 1, 0.3 and 0.05 μm alumina slurry, and then successively washed with diluted nitric acid, acetone and distilled water in ultrasonic bath, respectively. The original solution containing nanoplates (ca. 15mL) was concentrated to 1 mL, and then 100 μL of the condensed solution was dropped onto the pretreated GCE and dried in the air. After that, 4 μL Nafion (0.1%) was cast onto the electrode. Such modified electrode was used for electrochemical characterization. The modified electrode was stored at 4 $^{\circ}\text{C}$ when not used.

Instrumentation. UV-vis absorption spectra were taken using a JASCO V-570 spectrophotometer. The Transmission electron microscopy (TEM), high resolution transmission electron microscopy (HRTEM) and selected area electron diffraction (SAED) characterization was performed on

JEOL JEM-2100 electron microscopes with an operating voltage of 200 kV. Digital HRTEM images were analyzed to determine the crystalline of nanoplates by using digital micrograph 3.7. Atomic force microscopy (AFM) images were generated with a Veeco Multimodel NanoScope 3D in the tapping AFM mode. All electrochemical experiments were performed on a CHI 750E electrochemical workstation (CH Instruments, Chenhua Co., Shanghai, China). A conventional three-electrode system was employed with a modified GCE (3.0mm in diameter) as working electrode, a platinum sheet as auxiliary electrode and a saturated calomel electrode(SCE) as reference electrode.

Results and Discussion

Firstly, the sample of folding or rolling nanoplate is prepared at 70 $\mu\text{L}/\text{min}$ based on our previous report. The detailed morphology of the sample was characterized before.⁴³ Figure 1a and Figure S3(a-e) show clearly that the well-defined nanoplates are rolling or folding to different extent. Also, a thickness of about 1 nm could be predominantly seen from the rolling edge of the nanoplate (Fig. S3b). The HRTEM image of an individual nanoplate (Fig.1b) displays clear lattice fringes with fringe spacing about 0.235 nm, indicating that the entire nanoplate is crystalline with the (111) facet running across the main surface of nanoplate. The SAED pattern (Fig. 1c) shows a set of diffraction spots indexed to (111), (200), (220), (311) and (222) reflections of the gold *fcc* structure. The

UV–vis spectrum (Fig. 1d) shows a relatively narrow absorption band with the maximum absorption at about 590 nm, revealing that rolling nanoplates have a relatively uniform size.⁴⁰

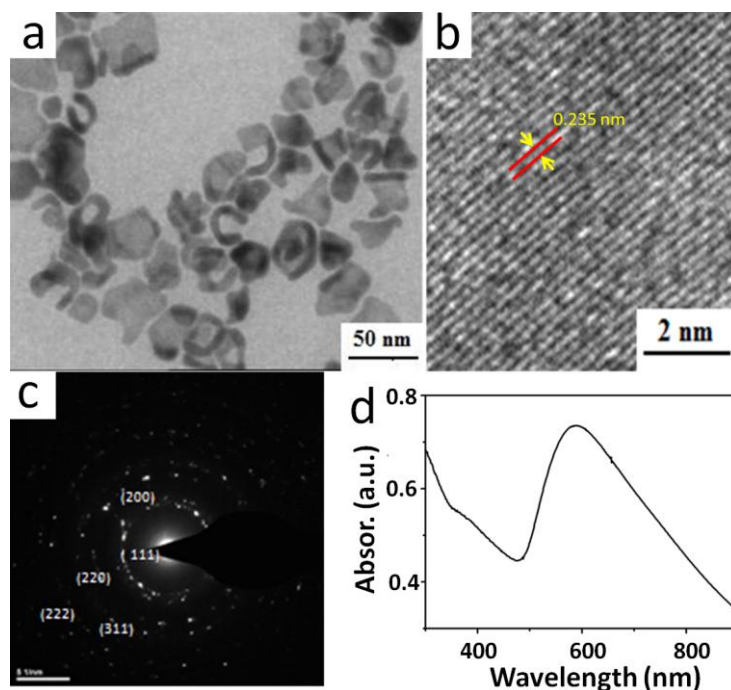


Fig. 1. (a) Typical TEM image of rolling Au nanoplates. (b) Typical HRTEM image of the surface of a Au nanoplate shown in (a). (c) Correlated SAED pattern for sample shown in (a). (d) Absorption spectra of ultrathin crumple gold nanoplates shown in (a).

Furthermore, to investigate the mechanism of such a rapid growth process, a series of microfluidic experiments at different flow rates were performed (Data shown in Fig.S4). To our surprise, it can be concluded that the rolling ultrathin gold nanoplates mentioned before can be obtained at a relatively high flow rates, while, at a low rate, the rigid surface-flat nanoplates could be obtained. Fig.2a and Fig.2b show that the products acquired at $5\mu\text{L}/\text{min}$ are just the rigid nanoplates with the fringe spacing of 0.235 nm (indexed to (111) facet), consistent with that of the

rolling nanoplate shown in Fig. 1b. Atomic force microscope (AFM) was utilized to certify the thickness of rigid nanoplates. As shown in Fig. 2c and Fig. 2d, the thickness of the nanoplates obtained with flow rate of $5\mu\text{L}/\text{min}$ is about 5.5 nm, which is much thicker than that ($< 1\text{nm}$) prepared at $70\mu\text{L}/\text{min}$ mentioned above (HRTEM image shown in Fig. S3b). Also, the sample gained at $5\mu\text{L}/\text{min}$ is thicker than the surface-flat sample (with thickness $\sim 2.5\text{ nm}$) prepared at $10\mu\text{L}/\text{min}$ (Fig. S5). In addition, AFM was also used to characterize the sample prepared at 30 and $50\mu\text{L}/\text{min}$. Unfortunately, the exact height of rolling nanoplates can't be measured directly by AFM due to their complicated rolling mode (Fig. S6). Based on these facts, we can conclude that, when the flow rate is low, the nanoplates could grow thick due to a long growth time before they flowed out from the chip and then were quenched by the ice water in the tube shown in Scheme 1. While when the flow rate is higher and higher, the growth time becomes shorter and shorter which then leads to thinner Au nanoplates. When it is thin enough, it tends to roll up to reduce the high surface energy.

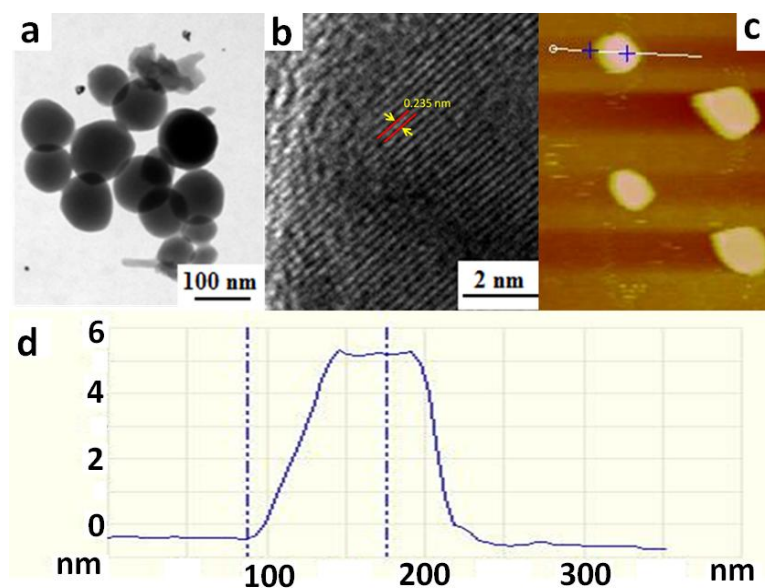


Fig. 2 (a) Typical TEM image of surface-flat Au nanoplates prepared at the rate of 5 $\mu\text{L}/\text{min}$, (b) typical HRTEM image of the surface of a nanoplate shown in (a), (c) typical AFM image of sample shown in (a), and (d) height profile along the colored line of a rigid gold nanoplate shown in (c).

Glucose oxidation in a phosphate buffered electrolyte is used to produce electricity in fuel cells and similar experimental conditions are adopted here to evaluate the electrocatalytic activities of different gold nanoplates. Before that, GCE modified by the rolling (red curve) and rigid (black curve) nanoplate were tested in 0.5M H_2SO_4 . As shown in Fig. 3a, the cyclic voltammetry (CV) curves show that the rolling nanoplate (obtained with flow rate of 70 $\mu\text{L}/\text{min}$) modified electrode displays much higher peak current associated with surface oxide reduction event than that of the rigid ones. Therefore, it is expected that the rolling nanoplates may have better performance in electrochemical oxidation of glucose than the rigid surface-flat nanoplates. Fig. 3b shows CV curves for glucose oxidation in a phosphate buffered solution on these

two modified GCEs. Two main regions can be observed. The first region is at 0.2 V vs SCE, an oxidation peak (peak A, which can't be seen clearly in the rolling nanoplate modified GCE), which is assigned to the dehydrogenation of the anomeric carbon of the glucose molecule. The current corresponding to this process is higher for rolling nanoplates than rigid ones. This dehydrogenation leads to the formation of gluconolactone. The second region presents the main oxidation peak centered at around 0.3 V vs SCE. (peak B), which corresponds to the further oxidation of gluconolactone.^{44, 45} Compared with that of the rigid nanoplate modified GCE, the rolling nanoplate modified GCE exhibited much larger oxidation currents, which clearly demonstrate the better electrocatalytic activity of the rolling nanoplates towards the glucose oxidation than the rigid ones. Also, the electrocatalytic activities of gold nanoplates prepared at 10 μ L/min, 30 μ L/min and 50 μ L/min was evaluated. As shown in Fig.S7, Their electrocatalytic activity are between that of rigid nanoplates(prepared at 5 μ L/min) and rolling nanoplates (prepared at 70 μ L/min). Meanwhile, their electrocatalytic activity are increased with the increasing flow rate(shown in Fig.S7).

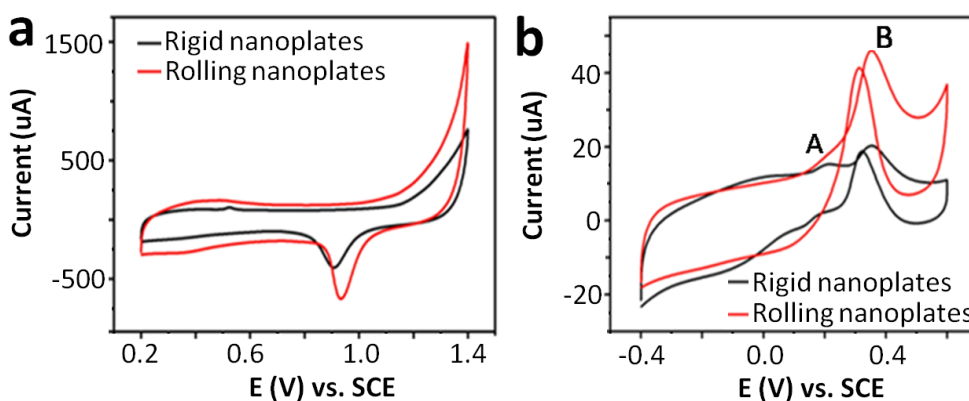


Fig.3. (a) The cyclic voltammograms of two types of (rigid/rolling) nanoplates modified electrodes in (a) 0.5 M H₂SO₄, (b) in PBS (pH7.4) in presence of 10 mM glucose recorded at 50 mV s⁻¹ and at 20 °C.

Meanwhile, electrodeposition method is one of the mostly useful approaches to prepare various types of gold nanostructures such as nanorod,^{46, 47} nanocube,⁴⁸ spherical nanoparticle⁴⁹ and so on. Nanoparticles with different shapes and sizes can be facily synthesized on the conducting surfaces by altering the conditions of electrochemical deposition. It is benefit to synthesize the hybrid material.⁵⁰⁻⁵² Isolated nanoparticle has to be acquired by additional separation process.⁴⁶ As for the microfluidic-based method, a higher surface to volume ratio and less sample consumption enable the chemical reaction processing in a continuous model within short time and giving a relatively uniform reaction environment.³⁵⁻³⁹ Moreover, microfluidic protocols offer the capability to automate multi-step synthesis with less human operation.

Conclusions

We have developed a continuous seed-mediated method for the preparation of high-purity gold nanoplates with tunable thickness, which

are rolling or rigid depending on their sizes. These nanoplates are poly-crystalline with different crystal faces and show a great electrochemical activity toward glucose oxidation. This protocol is fast, reproducible and adaptable to microfluidic synthesis without any additional batch processing steps, and probably could be extended to the synthesis of other types of ultrathin nanoplates.

Acknowledgment. This work was funded by the National Basic Research Program of China (973 Program, 2012CB932800 and 2014CB932700), National Natural Science Foundation of China (21273220 and 21422307), and “the Recruitment Program of Global youth Experts” of China.

References:

1. Y. Xia and N. J. Halas, *MRS Bulletin*, 2005, 30, 338-348.
2. C. J. Murphy, *Science*, 2002, 298, 2139-2141.
3. P. V. Kamat, *The Journal of Physical Chemistry B*, 2002, 106, 7729-7744.
4. M. A. El-Sayed, *Accounts of Chemical Research*, 2001, 34, 257-264.
5. N. R. Jana, L. Gearheart and C. J. Murphy, *Advanced Materials*, 2001, 13, 1389.
6. B. Nikoobakht and M. A. El-Sayed, *Chemistry of Materials*, 2003, 15, 1957-1962.
7. C. Wang and S. Sun, *Chemistry—An Asian Journal*, 2009, 4, 1028-1034.
8. H. Feng, Y. Yang, Y. You, G. Li, J. Guo, T. Yu, Z. Shen, T. Wu and B. Xing, *Chemical Communications*, 2009, 1984-1986.
9. J. Zhang, J. Du, B. Han, Z. Liu, T. Jiang and Z. Zhang, *Angewandte Chemie International Edition*, 2006, 45, 1116-1119.
10. N. Zhao, Y. Wei, N. Sun, Q. Chen, J. Bai, L. Zhou, Y. Qin, M. Li and L. Qi, *Langmuir*, 2008, 24, 991-998.
11. R. Jin, Y. Cao, C. A. Mirkin, K. Kelly, G. C. Schatz and J. Zheng, *Science*, 2001, 294, 1901-1903.
12. A. Miranda, E. Malheiro, E. Skiba, P. Quaresma, P. A. Carvalho, P. Eaton, B. de Castro, J. A. Shelnett and E. Pereira, *Nanoscale*, 2010, 2, 2209-2216.
13. F. Kim, S. Connor, H. Song, T. Kuykendall and P. Yang, *Angewandte Chemie International Edition*, 2004, 43, 3673-3677.
14. D. Seo, C. I. Yoo, J. C. Park, S. M. Park, S. Ryu and H. Song, *Angewandte Chemie International Edition*, 2008, 47, 763-767.
15. G. H. Jeong, M. Kim, Y. W. Lee, W. Choi, W. T. Oh, Q. H. Park and S. W. Han, *Journal of the*

- American Chemical Society*, 2009, 131, 1672-1673.
16. C. Li, K. L. Shuford, M. Chen, E. J. Lee and S. O. Cho, *ACS Nano*, 2008, 2, 1760-1769.
 17. M. S. Yavuz, W. Li and Y. Xia, *Chemistry – A European Journal*, 2009, 15, 13181-13187.
 18. S. E. Skrabalak, J. Chen, Y. Sun, X. Lu, L. Au, C. M. Cobley and Y. Xia, *Accounts of Chemical Research*, 2008, 41, 1587-1595.
 19. N. Zhao, L. Li, T. Huang and L. Qi, *Nanoscale*, 2010, 2, 2418-2423.
 20. H.-G. Liao, Y.-X. Jiang, Z.-Y. Zhou, S.-P. Chen and S.-G. Sun, *Angewandte Chemie International Edition*, 2008, 47, 9100-9103.
 21. P. S. Kumar, I. Pastoriza-Santos, B. Rodriguez-Gonzalez, F. J. G. de Abajo and L. M. Liz-Marzan, *Nanotechnology*, 2008, 19, 015606.
 22. S. Barbosa, A. Agrawal, L. Rodríguez-Lorenzo, I. Pastoriza-Santos, R. n. A. Alvarez-Puebla, A. Kornowski, H. Weller and L. M. Liz-Marzán, *Langmuir*, 2010, 26, 14943-14950.
 23. P. R. Sajanlal and T. Pradeep, *Nano Research*, 2009, 2, 306-320.
 24. Z. Wang, J. Zhang, J. M. Ekman, P. J. Kenis and Y. Lu, *Nano letters*, 2010, 10, 1886-1891.
 25. Y. Qin, Y. Song, N. Sun, N. Zhao, M. Li and L. Qi, *Chemistry of Materials*, 2008, 20, 3965-3972.
 26. T. Huang, F. Meng and L. Qi, *Langmuir*, 2009, 26, 7582-7589.
 27. X. Xu, J. Jia, X. Yang and S. Dong, *Langmuir*, 2010, 26, 7627-7631.
 28. W. Ye, J. Yan, Q. Ye and F. Zhou, *The Journal of Physical Chemistry C*, 2010, 114, 15617-15624.
 29. H. HianáTeo, *Chemical Communications*, 2010, 46, 7112-7114.
 30. S. E. Lohse, J. R. Eller, S. T. Sivapalan, M. R. Plews and C. J. Murphy, *ACS Nano*, 2013, 7, 4135-4150.
 31. D. Kumar, A. Kulkarni and B. Prasad, *Colloids and Surfaces A: Physicochemical and Engineering Aspects*, 2014, 443, 149-155.
 32. C. Bullen, M. J. Latter, N. J. D'Alonzo, G. J. Willis and C. L. Raston, *Chemical Communications*, 2011, 47, 4123-4125.
 33. V. Sebastián, S.-K. Lee, C. Zhou, M. F. Kraus, J. G. Fujimoto and K. F. Jensen, *Chemical Communications*, 2012, 48, 6654-6656.
 34. J. Boleinger, A. Kurz, V. Reuss and C. Sönnichsen, *Physical Chemistry Chemical Physics*, 2006, 8, 3824-3827.
 35. C.-H. Weng, C.-C. Huang, C.-S. Yeh, H.-Y. Lei and G.-B. Lee, *Journal of Micromechanics and microengineering*, 2008, 18, 035019.
 36. V. Sebastian Cabeza, S. Kuhn, A. A. Kulkarni and K. F. Jensen, *Langmuir*, 2012, 28, 7007-7013.
 37. L. L. Lazarus, A. S.-J. Yang, S. Chu, R. L. Brutchey and N. Malmstadt, *Lab Chip*, 2010, 10, 3377-3379.
 38. D. Shalom, R. C. Wootton, R. F. Winkle, B. F. Cottam, R. Vilar and C. P. Wilde, *materials Letters*, 2007, 61, 1146-1150.
 39. J. Wagner and J. M. Köhler, *Nano Letters*, 2005, 5, 685-691.
 40. S. Yang, T. Zhang, L. Zhang, S. Wang, Z. Yang and B. Ding, *Colloids and Surfaces A: Physicochemical and Engineering Aspects*, 2007, 296, 37-44.
 41. Y. Shao, Y. Jin and S. Dong, *Chem. Commun.*, 2004, 1104-1105.
 42. B. Cao, B. Liu and J. Yang, *CrystEngComm*, 2013, 15, 5735-5738.
 43. Q. Fu, Y. Sheng, H. Tang, Z. Zhu, M. Ruan, W. Xu, Y. Zhu and Z. Tang, *ACS Nano*, 2015, DOI: 10.1021/nn5027998.
 44. M. Pasta, F. La Mantia and Y. Cui, *Electrochimica Acta*, 2010, 55, 5561-5568.

45. J. Wang, J. Gong, Y. Xiong, J. Yang, Y. Gao, Y. Liu, X. Lu and Z. Tang, *Chemical Communications*, 2011, 47, 6894-6896.
46. B. M. I. van der Zande, M. R. Böhmer, L. G. J. Fokkink and C. Schönenberger, *Langmuir*, 2000, 16, 451-458.
47. B. M. Van der Zande, M. R. Böhmer, L. G. Fokkink and C. Schönenberger, *The Journal of Physical Chemistry B*, 1997, 101, 852-854.
48. J. Hernández, J. Solla-Gullón, E. Herrero, A. Aldaz and J. M. Feliu, *The Journal of Physical Chemistry C*, 2007, 111, 14078-14083.
49. H. Zhang, J.-J. Xu and H.-Y. Chen, *The Journal of Physical Chemistry C*, 2008, 112, 13886-13892.
50. J. C. Claussen, M. M. Wickner, T. S. Fisher and D. M. Porterfield, *ACS applied materials & interfaces*, 2011, 3, 1765-1770.
51. Y. Hu, J. Jin, P. Wu, H. Zhang and C. Cai, *Electrochimica Acta*, 2010, 56, 491-500.
52. A. D. Franklin, D. B. Janes, J. C. Claussen, T. S. Fisher and T. D. Sands, *Applied Physics Letters*, 2008, 92, 013122.